



Cite this: *Chem. Commun.*, 2016, 52, 7802

Received 10th March 2016,  
Accepted 9th May 2016

DOI: 10.1039/c6cc02142e

www.rsc.org/chemcomm

## 13-Helix folding of a $\beta/\gamma$ -peptide manifold designed from a “minimal-constraint” blueprint†

Claire M. Grison,<sup>a</sup> Sylvie Robin<sup>ab</sup> and David J. Aitken<sup>\*a</sup>

**A bottom-up design rationale was adopted to devise  $\beta/\gamma$ -peptide foldamer manifolds which would adopt preferred 13-helix conformations, relying on minimal steric imposition brought by the constituent amino acid residues. In this way, a well-defined 13-helix conformer was revealed for short oligomers of *trans*-2-aminocyclobutanecarboxylic acid and  $\gamma^4$ -amino acids in alternation, which gave good topological superposition upon an  $\alpha$ -helix motif.**

Peptide oligomers which fold regularly around an intramolecular network of non-covalent interactions, principally hydrogen bonds (H-bonds), have been at the forefront of foldamer science since their inception and remain of primary importance today. Through the construction of different sequences of homo- and hetero-oligopeptides containing non-canonical  $\beta$ - or  $\gamma$ -amino acid building blocks, a widely-varied collection of folded conformations has been established.<sup>1</sup>

The design of particular types of foldamer architecture is a contemporary challenge and one major objective is the preparation of  $\alpha$ -helix mimetics. In native proteins,  $\alpha$ -helices play a structural role when buried in the hydrophobic core, serving to stabilise the tertiary structure. When completely or partially exposed on the surface of proteins,  $\alpha$ -helices play critical roles in the interactions of proteins with other biological molecules.<sup>2</sup> In the search for mediators of protein–protein interactions, a number of approaches to develop  $\alpha$ -helix mimetics have been considered,<sup>3</sup> and some notable successes have been described by employing  $\beta$ -peptide<sup>4</sup> or  $\alpha/\beta$ -peptide<sup>5</sup> foldamers which adopt helical architectures. For example, Schepartz has elaborated helical  $\beta$ -peptides which can present “hot-spot” side chains along one face, leading to the development of inhibitors of targeted

protein–protein interactions,<sup>6</sup> inhibitors of HIV fusion,<sup>7</sup> and agonists of a particular G protein-coupled receptor.<sup>8</sup>

The  $\beta/\gamma$ -hybrid peptide manifold is of special interest because a  $\beta/\gamma$ -dipeptide has the same number of backbone atoms as a native  $\alpha$ -tripeptide. Indeed, in a seminal theoretical study, Hofmann suggested that the 13-helix of a  $\beta/\gamma$ -peptide might exhibit the same dipole and H-bond orientations as the  $\alpha$ -helix.<sup>9</sup> Successful isosteric replacements of short  $\alpha$ -helical segments by  $\beta/\gamma$ -peptide fragments in  $\alpha$ -peptides have been described.<sup>10</sup> Recently, a study of single side-chain  $\beta^3$ - and  $\gamma^4$ -amino acid insertion into short helical  $\alpha$ -peptides revealed that the latter residues were more propitious for helical folding.<sup>11</sup> However, with flexible  $\beta/\gamma$ -peptides a number of stable conformations are accessible, including a 11/13-helix<sup>12</sup> and a non-helical 9/8-ribbon.<sup>13</sup> Balaram observed a cyclic 13-membered ring (C13) H-bond feature in selected  $\beta,\gamma$ -tripeptides.<sup>14</sup> To date, only one description of a 13-helical  $\beta/\gamma$ -peptide has been reported: Gellman successfully imposed the requisite secondary structure by applying draconian steric constraints upon each constituent residue.<sup>15</sup> While this work was a proof-of-principle milestone, the opportunities for the introduction of functional side chains are limited due to the severe steric hindrance in operation.

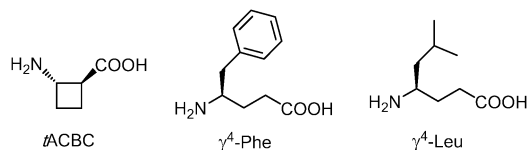
Given the particular attraction of the  $\beta/\gamma$ -peptide 13-helix as a potential  $\alpha$ -helix mimetic, we sought to establish a “minimal constraint” axiom with low steric congestion for this secondary structure. Hofmann’s prediction for a stable, right-handed (*P*) 13-helix implicates a backbone  $\theta$  torsion angle in the range 90° to 100° for the  $\beta$ -residue component and  $g^+$ ,  $g^+$  local conformations for the  $\gamma$ -residues. Following a bottom-up design rationale to accommodate these criteria, we reasoned that a suitable  $\beta$ -amino acid component would be the small, constrained *trans*-(1*S*,2*S*)-2-aminocyclobutanecarboxylic acid (*tACBC*),<sup>16</sup> whose homo-oligomers support a robust 12-helix.<sup>17</sup> Unsubstituted  $\gamma$ -aminobutyric acid (GABA) was disfavoured as the  $\gamma$ -component, since it facilitates 9/8-ribbon formation;<sup>13</sup> we selected instead a singly substituted (*R*)- $\gamma^4$ -amino acid. The inclusion of a substituent is in fact pertinent, if the target 13-helix is to provide recognizable side chains on its periphery.

<sup>a</sup> CP3A Organic Synthesis Group, ICMO, UMR 8182, CNRS, Université Paris-Sud, Université Paris-Saclay, 15 Rue Georges Clemenceau, 91405 Orsay cedex, France. E-mail: david.aitken@u-psud.fr; Fax: +33-(0)169156278; Tel: +33-(0)169153238

<sup>b</sup> Université Paris Descartes, UFR Sciences Pharmaceutiques et Biologiques, 4 Avenue de l’Observatoire, 75270 Paris cedex 06, France

† Electronic supplementary information (ESI) available: Synthetic procedures, CD, IR and NMR analyses, and molecular modelling data. See DOI: 10.1039/c6cc02142e





- 1 Boc- $t\text{ACBC}$ - $\gamma^4\text{-Phe}$ - $t\text{ACBC}$ - $\gamma^4\text{-Leu}$ -OBn
- 2 Boc- $t\text{ACBC}$ - $\gamma^4\text{-Phe}$ - $t\text{ACBC}$ - $\gamma^4\text{-Leu}$ -NHBN
- 3 Boc- $\gamma^4\text{-Phe}$ - $t\text{ACBC}$ - $\gamma^4\text{-Leu}$ - $t\text{ACBC}$ -OBn
- 4 Boc- $\gamma^4\text{-Phe}$ - $t\text{ACBC}$ - $\gamma^4\text{-Leu}$ - $t\text{ACBC}$ -NHBN
- 5 Boc- $t\text{ACBC}$ - $\gamma^4\text{-Phe}$ - $t\text{ACBC}$ - $\gamma^4\text{-Phe}$ - $t\text{ACBC}$ -OBn
- 6 Boc- $t\text{ACBC}$ - $\gamma^4\text{-Phe}$ - $t\text{ACBC}$ - $\gamma^4\text{-Phe}$ - $t\text{ACBC}$ -NHBN
- 7 Boc- $\gamma^4\text{-Phe}$ - $t\text{ACBC}$ - $\gamma^4\text{-Phe}$ - $t\text{ACBC}$ - $\gamma^4\text{-Leu}$ -OBn
- 8 Boc- $\gamma^4\text{-Phe}$ - $t\text{ACBC}$ - $\gamma^4\text{-Phe}$ - $t\text{ACBC}$ - $\gamma^4\text{-Leu}$ -NHBN
- 9 Boc- $t\text{ACBC}$ - $\gamma^4\text{-Phe}$ - $t\text{ACBC}$ - $\gamma^4\text{-Phe}$ - $t\text{ACBC}$ - $\gamma^4\text{-Leu}$ -OBn
- 10 Boc- $t\text{ACBC}$ - $\gamma^4\text{-Phe}$ - $t\text{ACBC}$ - $\gamma^4\text{-Phe}$ - $t\text{ACBC}$ - $\gamma^4\text{-Leu}$ -NHBN
- 11 Boc- $\gamma^4\text{-Phe}$ - $t\text{ACBC}$ - $\gamma^4\text{-Phe}$ - $t\text{ACBC}$ - $\gamma^4\text{-Leu}$ - $t\text{ACBC}$ -OBn
- 12 Boc- $\gamma^4\text{-Phe}$ - $t\text{ACBC}$ - $\gamma^4\text{-Phe}$ - $t\text{ACBC}$ - $\gamma^4\text{-Leu}$ - $t\text{ACBC}$ -NHBN

Fig. 1 Monomer  $\beta$ - and  $\gamma$ -amino acid residues and sequences of  $\beta/\gamma$ -peptides 1–12.

To test this hypothesis we prepared twelve  $\beta/\gamma$ -peptides, 1–12, for study. The monomer building blocks and the peptide sequences are presented in Fig. 1. The  $\gamma$ -residues, (*R*)- $\gamma^4\text{-Phe}$  and (*R*)- $\gamma^4\text{-Leu}$ , were selected to resemble hydrophobic  $\alpha$ -residues which should not interfere with the backbone H-bonding preferences. The features which were varied within this series were the sequence length (tetra-, penta- and hexa-peptides); the N-terminal residue (*t*ACBC or a  $\gamma^4$ -amino acid); and the nature of the C-terminal capping group (ester or amide). The twelve peptides were synthesised using standard solution-state peptide coupling techniques (see the ESI†).

All  $^1\text{H}$  and  $^{13}\text{C}$  NMR spectroscopic signals pertinent to conformational analysis were unambiguously assigned to each peptide using standard 1D and 2D pulse sequences in  $\text{CDCl}_3$ . Titration of the  $\text{CDCl}_3$  solutions with  $\text{DMSO}-d_6$  revealed a higher titration coefficient for the carbamate and amide NH signals of residues 1 and 2, respectively, than for the other NH signals in each peptide, suggesting that the former NH functions were at least partially solvent exposed and not extensively engaged in hydrogen bonding. This initial observation was qualitatively encouraging, since the folding of the desired 13-helix conformer should not implicate either of the first two NH functions.

Conformational analysis of all twelve peptides 1–12 was carried out using ROESY NMR experiments in  $\text{CDCl}_3$  solution; interpretation of the data was corroborated by molecular modelling conducted in the form of a hybrid Monte Carlo molecular mechanics (MCMC) conformation search carried out in chloroform medium, using MacroModel and the MMFF force field without restraints. From 10 000 generated structures the lowest energy conformers ( $<20 \text{ kJ mol}^{-1}$ ) were retained and sorted according to their conformer family type (see the ESI†).

In the analysis of tetrapeptides 1–4, short range hydrogen-bonding emerged as the main feature of a rather complex conformational landscape. In each case, ROESY experiments showed short range  $\text{H}\alpha(i)\text{-NH}(i+1)$  and  $\text{H}\beta(i)\text{-NH}(i+1)$  correlations around one or both *t*ACBC residues, as well as  $\text{H}\gamma(i)\text{-NH}(i+1)$

correlations around one or both  $\gamma^4$ -amino acid residues. These phenomena are diagnostic of C8 and C9 H-bonding features, which form the basis of a 9/8-ribbon.<sup>13</sup> The molecular modelling survey confirmed that the 9/8-ribbon was the most common folded conformer in all four peptides.

Longer distance ROESY  $\text{H}\gamma(i)\text{-NH}(i+2)$  correlations were observed for 2, 3 and 4, as well as  $\text{H}\beta(i)\text{-NH}(i+2)$  and  $\text{H}\beta(i)\text{-H}\alpha(i+2)$  correlations for 3 and 4. These observations were supportive of C13 H-bonds;<sup>15</sup> however molecular modelling suggested that the “all-C13” conformers, corresponding to 13-helix structures, were accompanied by mixed conformers featuring combinations of C13 and C8 and/or C9 interactions.

ROESY data for pentapeptides 5–8 featured the propitious long distance correlations  $\text{H}\gamma(i)\text{-NH}(i+2)$ ,  $\text{H}\beta(i)\text{-NH}(i+2)$  and  $\text{H}\beta(i)\text{-H}\alpha(i+2)$ , which are diagnostic for conformers having C13 H-bonding. Furthermore, previously-undescribed  $\text{H}\gamma(i)\text{-NH}(i+3)$  correlations were observed in 5 and 8 (two such correlations for the latter), which were fully consistent with a 13-helix structure. Molecular modelling suggested that 13-helix conformers were dominant for peptides 5 and 8 and made significant contributions to peptides 6 and 7. In all of the low-energy conformers of the latter two peptides, at least two consecutive C13 features were present. The short-range (*i*)-(*i*+1) ROESY correlations shown by these compounds are an integral part of the C13 ROESY signature, rather than being indicative of the presence of alternative C8 or C9 H-bonded conformers.

The four hexapeptides 9–12 provided extensive ROESY correlation data which were entirely consistent with a dominant 13-helix conformer in each case. For hexapeptide ester 9, the presence of a second conformer was suspected, in which the C-terminal of the 13-helix had given way to the C8 feature around *t*ACBC-5. Molecular modelling suggested that in fact, for all four peptides, minor contributions might arise from N- or C-terminal “tightening” of the H-bonding pattern; however the 13-helix essentially remained the central feature of the conformer landscape. Fig. 2 shows the ROESY correlations observed for peptides 9–12 along with the 13-helix H-bonding networks deduced from these data.

The solution-state IR absorption spectra of peptides 1–12 in chloroform (see the ESI†) confirmed the general trends for the folding predilection described above. In all cases, free carbamate (residue 1) and amide (residue 2) NH vibrations appeared in the region of  $3430\text{--}3450 \text{ cm}^{-1}$ . For peptides 1–4, low frequency (H-bonded) amide NH bands were discernible at around  $3260 \text{ cm}^{-1}$  for C8 motifs and at around  $3350 \text{ cm}^{-1}$  for C9 motifs. For pentapeptides 5–8, these features were less well defined and the curves evolved towards increased absorption in the zone between these two frequencies, concomitant with significant C13 contributions. For peptides 9–12 the most intense absorption was in the region at around  $3310 \text{ cm}^{-1}$ , in agreement with the predominance of 13-helix conformers. It is noteworthy that the 12-helix formed by homo-oligomers of *t*ACBC has a C12 H-bonded amide NH absorption centred at  $3300 \text{ cm}^{-1}$  in the same solvent.<sup>17</sup>

The peptides considered here were insoluble in water. The far-UV circular dichroism (CD) spectra were recorded in MeOH



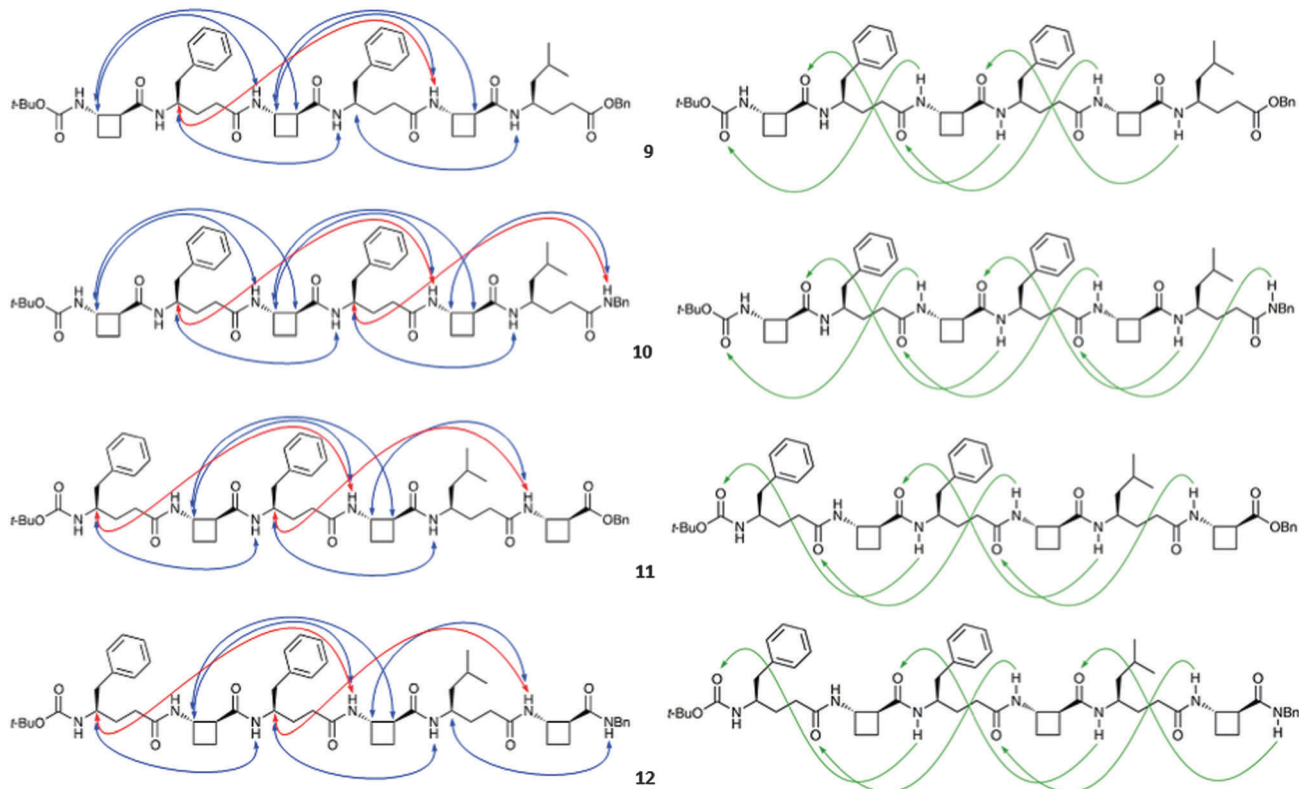


Fig. 2 Characteristic ROESY correlations (left) and 13-helix H-bonding patterns (right) of  $\beta/\gamma$ -peptides **9–12** observed in  $\text{CDCl}_3$  (10 mM). Short range correlations have been omitted from the left panel for clarity.

(0.20 mM) for the pentapeptides and hexapeptides **5–12**, which showed a considerable or substantial population of 13-helix conformers. The common features show a small positive Cotton effect at around 225 nm and a stronger negative Cotton effect at 206 nm, with a mean-residue ellipticity  $[\theta]$  reaching a significant value of  $25 \times 10^3 \text{ deg cm}^2 \text{ dmol}^{-1}$  for the latter (Fig. 3). While the CD spectrum of a  $\beta/\gamma$ -peptide 13-helix has been neither calculated nor reported, these data are very close to the CD signature of a right-handed  $\beta$ -peptide 12-helix in the same

solvent.<sup>17,18</sup> This observation is entirely consistent with the prevalence of the  $\beta/\gamma$ -peptide 13-helix conformer in polar protic solution.

The 13-helix conformers generated by the MCMM conformational search for each of the four hexapeptides **9–12** were subjected to *ab initio* geometry optimization by DFT using GAUSSIAN 09 and the B3LYP/6-311G(d,p) basis set in chloroform medium (Fig. 4) (for details, see the ESI†).

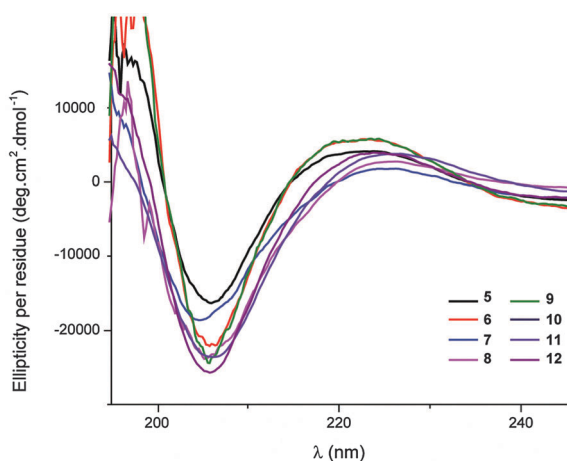


Fig. 3 CD spectra of  $\beta/\gamma$ -peptides **5–12** in MeOH (0.20 mM).

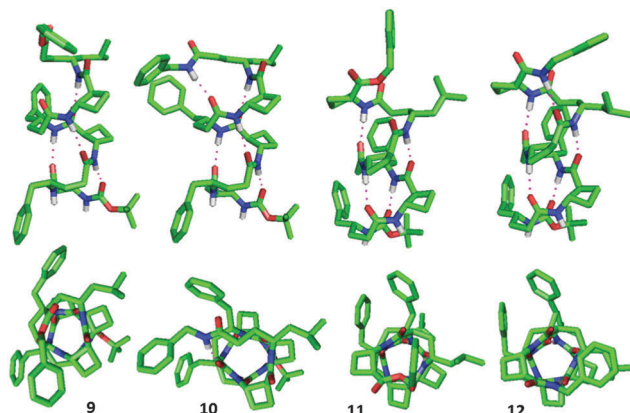


Fig. 4 Side-views (upper panel) and top-views (lower panel) of the low energy conformers of  $\beta/\gamma$ -peptides **9–12** showing a 13-helical conformation. Hydrogen atoms not relevant to H-bonding have been removed from the images for clarity.





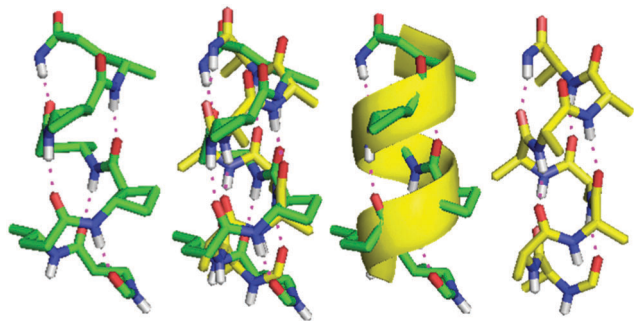


Fig. 5 Comparison of the 13-helix adopted by  $\beta/\gamma$ -peptide **10** (left) and the right-handed  $\alpha$ -helix of oligo-Ala (right). For clarity, only the H-bonded part of the peptide backbone and directly-bound atoms are shown. The superposition of the two helices is shown directly (centre left) and with the  $\alpha$ -helix represented as a yellow ribbon (centre right).

Four (for peptides **9** and **11**) or five (for peptides **10** and **12**) standard hydrogen bonds form the basis of the right-handed (*P*) 13-helical structures, displaying C=O $\cdots$ H-N distances within the range of 1.78 Å to 2.01 Å and O $\cdots$ H-N angles within the range of 169.7° to 178.9°. In all peptides, the  $\gamma^4$ -amino acid residues each adopted the anticipated  $g^+$ ,  $g^+$  conformations, showing  $\theta$  and  $\zeta$  torsion angles falling in the ranges of 44° to 62° and 56° to 63°, respectively, for those residues which were involved in the H-bonding network. For the *t*ACBC residues the backbone  $\theta$  torsion angle values fell within the narrow range of 100° to 106°, which was close to the  $\theta$  value ranges previously observed for *t*ACBC in an 8-helix foldamer (101° to 104°)<sup>19</sup> or a 9/8-ribbon (99° to 102°),<sup>13</sup> although perceptibly greater than the range observed for *t*ACBC in its homo-oligomeric 12-helix (96° to 100°).<sup>17</sup> However, when the  $\phi$  and  $\psi$  torsion angles (averaging around −102° and −106°, respectively) are taken into account, *t*ACBC approaches convincingly the idealized topology and pitch rise for the  $\beta$ -amino acid component in a  $\beta/\gamma$ -peptide 13-helix: the theoretical values for  $\phi$ ,  $\theta$  and  $\psi$  average around −96°, 94° and −115°, respectively, in Hofmann's idealized unconstrained model.<sup>9</sup>

The topology of the  $\beta/\gamma$ -peptide 13-helical backbone was compared with a model of the native  $\alpha$ -helical backbone based on oligo-Ala (Fig. 5). The 13-helix of peptide **10** and the  $\alpha$ -helix model pleasingly exhibited the same orientation of the helix dipole and close similarities in helix pitch and diameter.

In conclusion, the judicious combination of the small cyclic  $\beta$ -amino acid *t*ACBC and a singly-substituted  $\gamma^4$ -amino acid provides sufficient steric imposition to induce regular folding of a  $\beta/\gamma$ -peptide manifold into a well-defined 13-helix conformer. This secondary structure overlays very well with a representative  $\alpha$ -helical peptide; since its backbone is relatively unhindered, it may constitute a useful manifold for the design of mimetics of natural  $\alpha$ -helical fragments.

We are grateful to Mr J.-P. Baltaze (ICMMO) for help with NMR experiments. The award of a French MESR doctoral research scholarship (to C. M. G.) is acknowledged.

## Notes and references

- (a) *Foldamers: Structure, Properties, and Applications*, ed. S. Hecht and I. Huc, Wiley-VCH Verlag GmbH & Co, Weinheim, 2007; (b) G. Guichard and I. Huc, *Chem. Commun.*, 2011, **47**, 5933; (c) D. J. Hill, M. J. Mio, R. B. Prince, T. S. Hughes and J. S. Moore, *Chem. Rev.*, 2001, **101**, 3893; (d) T. A. Martinek and F. Fülöp, *Chem. Soc. Rev.*, 2012, **41**, 687; (e) P. G. Vasudev, S. Chatterjee, N. Shamala and P. Balaram, *Chem. Rev.*, 2011, **111**, 657; (f) A. Roy, P. Prabhakaran, P. K. Baruah and G. J. Sanjayan, *Chem. Commun.*, 2011, **47**, 11593; (g) W. S. Horne and S. H. Gellman, *Acc. Chem. Res.*, 2008, **41**, 1399; (h) D. Seebach, D. F. Hook and A. Glättli, *Biopolymers*, 2006, **84**, 23; (i) R. P. Cheng, S. H. Gellman and W. F. DeGrado, *Chem. Rev.*, 2001, **101**, 3219.
- (a) D. J. Barlow and J. M. Thornton, *J. Mol. Biol.*, 1988, **201**, 601; (b) T. E. Creighton, *Proteins: Structures and Molecular Properties*, W.H. Freeman & Co, New York, 2nd edn, 1992; (c) G. T. Kilosaniidze, A. S. Kutsenko, N. G. Esipova and V. G. Tumanyan, *Protein Sci.*, 2004, **13**, 351.
- (a) M. Pelay-Gimeno, A. Glas, O. Koch and T. N. Grossmann, *Angew. Chem., Int. Ed.*, 2015, **54**, 8896; (b) V. Azzarito, K. Long, N. S. Murphy and A. J. Wilson, *Nat. Chem.*, 2013, **5**, 161; (c) B. N. Bullock, A. L. Jochim and P. S. Arora, *J. Am. Chem. Soc.*, 2011, **133**, 14220; (d) J. Gardner and M. M. Harding, *Org. Biomol. Chem.*, 2007, **5**, 3577.
- M. Hintersteiner, T. Kimmerlin, G. Garavel, T. Schindler, R. Bauer, N.-C. Meisner, J.-M. Seifert, V. Uhl and M. Auer, *ChemBioChem*, 2009, **10**, 994.
- (a) R. W. Cheloha, A. Maeda, T. Dean, T. J. Gardella and S. H. Gellman, *Nat. Biotechnol.*, 2014, **32**, 653; (b) L. M. Johnson, S. Barrick, M. V. Hager, A. McFedries, E. A. Homan, M. E. Rabaglia, M. P. Keller, A. D. Attie, A. Saghatelian, A. Bisello and S. H. Gellman, *J. Am. Chem. Soc.*, 2014, **136**, 12848; (c) B. J. Smith, E. F. Lee, J. W. Checco, M. Evangelista, S. H. Gellman and W. D. Fairlie, *ChemBioChem*, 2013, **14**, 1564; (d) M. D. Boersma, H. S. Haase, K. J. Peterson-Kaufman, E. F. Lee, O. B. Clarke, P. M. Colman, B. J. Smith, W. S. Horne, W. D. Fairlie and S. H. Gellman, *J. Am. Chem. Soc.*, 2012, **134**, 315; (e) W. S. Horne, M. D. Boersma, M. A. Windsor and S. H. Gellman, *Angew. Chem., Int. Ed.*, 2008, **47**, 2853.
- (a) E. A. Harker and A. Schepartz, *ChemBioChem*, 2009, **10**, 990; (b) E. A. Harker, D. S. Daniels, D. A. Guarracino and A. Schepartz, *Bioorg. Med. Chem.*, 2009, **17**, 2038.
- O. M. Stephens, S. Kim, B. D. Welch, M. E. Hodsdon, M. S. Kay and A. Schepartz, *J. Am. Chem. Soc.*, 2005, **127**, 13126.
- E. V. Denton, C. J. Craig, R. L. Pongratz, J. S. Appelbaum, A. E. Doerner, A. Narayanan, G. I. Schulman, G. W. Cline and A. Schepartz, *Org. Lett.*, 2013, **15**, 5318.
- C. Baldauf, R. Günther and H.-J. Hofmann, *J. Org. Chem.*, 2006, **71**, 1200.
- (a) R. R. Araghi, C. Jäckel, R. Cölfen, M. Salwiczek, A. Völkel, S. C. Wagner, S. Wiczorek, C. Baldauf and B. Koksche, *ChemBioChem*, 2010, **11**, 335; (b) I. L. Karle, A. Pramanik, A. Bannerjee, S. Bhattacharjya and P. Balaram, *J. Am. Chem. Soc.*, 1997, **119**, 9087.
- Y.-H. Shin, D. E. Mortenson, K. A. Satyshur, K. T. Forest and S. H. Gellman, *J. Am. Chem. Soc.*, 2013, **135**, 8149.
- G. V. M. Sharma, V. B. Jadhav, K. V. S. Ramakrishna, P. Jayaprakash, K. Narsimulu, V. Subash and A. C. Kunwar, *J. Am. Chem. Soc.*, 2006, **128**, 14657.
- C. M. Grison, S. Robin and D. J. Aitken, *Chem. Commun.*, 2015, **51**, 16233.
- P. G. Vasudev, K. Ananda, S. Chatterjee, S. Aravinda, N. Shamala and P. Balaram, *J. Am. Chem. Soc.*, 2007, **129**, 4039.
- L. Guo, A. M. Almeida, W. Zhang, A. G. Reidenbach, S. H. Choi, I. A. Guzei and S. H. Gellman, *J. Am. Chem. Soc.*, 2010, **132**, 7868.
- (a) V. Declerck and D. J. Aitken, *Amino Acids*, 2011, **41**, 587; (b) C. Fernandes, E. Pereira, S. Faure and D. J. Aitken, *J. Org. Chem.*, 2009, **74**, 3217; (c) C. Fernandes, C. Gauzy, Y. Yang, O. Roy, E. Pereira, S. Faure and D. J. Aitken, *Synthesis*, 2007, 2222.
- C. Fernandes, S. Faure, E. Pereira, V. Théry, V. Declerck, R. Guillot and D. J. Aitken, *Org. Lett.*, 2010, **12**, 3606.
- (a) H.-S. Lee, F. A. Syud, X. Wang and S. H. Gellman, *J. Am. Chem. Soc.*, 2001, **123**, 7721; (b) X. Wang, J. F. Espinosa and S. H. Gellman, *J. Am. Chem. Soc.*, 2000, **122**, 4821.
- A. Altmayer-Henzien, V. Declerck, J. Farjon, D. Merlet, R. Guillot and D. J. Aitken, *Angew. Chem., Int. Ed.*, 2015, **54**, 10807.

